


Isomorphism Continuum Stored Energy Functional for Finite Thermoelastic Deformation

Fuzhang Zhao 

APD Optima Study, Lake Forest, CA, USA

Email: fuzhangzhao@yahoo.com

How to cite this paper: Zhao, F.Z. (2023) Isomorphism Continuum Stored Energy Functional for Finite Thermoelastic Deformation. *Advances in Pure Mathematics*, 13, 133-151.

<https://doi.org/10.4236/apm.2023.132007>

Received: January 30, 2023

Accepted: February 25, 2023

Published: February 28, 2023

Copyright © 2023 by author(s) and

Scientific Research Publishing Inc.

This work is licensed under the Creative

Commons Attribution International

License (CC BY 4.0).

<http://creativecommons.org/licenses/by/4.0/>



Open Access

Abstract

Continuum mechanics for isotropic finite thermoelastic deformations have been reviewed. Thermal effects on mechanical responses of rubbers have been captured by the isomorphism continuum stored energy (CSE) functional with the multiplicative decomposition of deformation gradient while preserving the structure of symmetry for finite structural deformation. The CSE finite thermoelastic model fits and predicts experimental data of SR and NR-C60 rubbers at different external temperatures. For internal temperature effects of both NR and NR-SIC rubbers, the CSE finite thermoelastic model of stored energy and entropy, along with the newly developed CTE and CI models, fits both nominal stress-stretch and temperature change-stretch experimental data in uniaxial extension tests.

Keywords

Entropy, Finite Thermoelasticity, Isomorphism Constitutive Model, Strain-Induced Crystallization, Thermodynamics

1. Introduction

General theories of thermoelasticity have been evolved over a long period of time. For constitutive modeling isotropic finite thermoelastic deformations of rubberlike materials, two fundamental methodologies: statistical mechanics and continuum mechanics have briefly been reviewed by Holzapfel and Simo (1996) [1]. In the approach of continuum mechanics, both classical and contemporary theories of thermoelasticity have been developed. Continuum constitutive modeling theories for isotropic finite thermoelastic deformations will briefly be studied.

Within the classical theory of thermoelasticity, constitutive models, stress-deformation-temperature relations, are formulated under the thermodynamic framework within two configurations: the initial unstressed referential configuration Ω_0 with uniform temperature and the current configuration Ω with non-uniform stress and temperature fields. The Clausius-Duhem form of the second law of thermodynamics leads to the following local imbalance

$$\mathcal{D}_{\text{int}} = \mathbf{S} : \frac{\dot{\mathbf{C}}}{2} - \dot{\Psi} - \eta \dot{\theta} - \frac{1}{\theta} \mathbf{q} \cdot \nabla \theta \geq 0, \quad (1)$$

where \mathcal{D}_{int} is the internal dissipation rate, \mathbf{S} is the second Piola-Kirchhoff stress tensor, $\dot{\mathbf{C}}$ is the rate of the right Cauchy-Green tensor, $\dot{\Psi}$ is the rate of a stored energy functional per unit reference volume, η is the entropy per unit reference volume, \mathbf{q} is the heat flux, θ is the absolute temperature, and $\dot{\theta}$ is the rate of an absolute temperature. As a stored energy function takes the form of $\Psi = \Psi(\mathbf{C}, \theta)$, its time derivative due to the chain rule of differentiation reads,

$$\dot{\Psi} = \frac{\partial \Psi}{\partial \mathbf{C}} : \dot{\mathbf{C}} + \frac{\partial \Psi}{\partial \theta} \dot{\theta}. \quad (2)$$

Substituting (2) into (1) and collecting terms gives

$$\mathcal{D}_{\text{int}} = \left(\mathbf{S} - 2 \frac{\partial \Psi}{\partial \mathbf{C}} \right) : \frac{\dot{\mathbf{C}}}{2} - \left(\eta + \frac{\partial \Psi}{\partial \theta} \right) \dot{\theta} - \frac{1}{\theta} \mathbf{q} \cdot \nabla \theta \geq 0. \quad (3)$$

For arbitrary $\dot{\mathbf{C}}$, $\dot{\theta}$, and θ , general constitutive relations are obtained

$$\mathbf{S} = 2 \frac{\partial \Psi}{\partial \mathbf{C}}, \quad \eta = - \frac{\partial \Psi}{\partial \theta}, \quad \mathbf{q} \cdot \nabla \theta \leq 0. \quad (4)$$

Taking the time derivatives of constitutive Equations (4)₁ and (4)₂ yields two rate equations

$$\mathbf{S} = \mathbb{C} : \frac{\dot{\mathbf{C}}}{2} - \boldsymbol{\zeta} \frac{\dot{\theta}}{\theta}, \quad \theta \dot{\eta} = \boldsymbol{\zeta} : \frac{\dot{\mathbf{C}}}{2} + \rho C \dot{\theta}, \quad (5)$$

and three important tangential measures, \mathbb{C} , $\boldsymbol{\zeta}$, and ρC , are defined as

$$\mathbb{C} = 4 \frac{\partial^2 \Psi}{\partial \mathbf{C} \partial \mathbf{C}}, \quad \boldsymbol{\zeta} = -2\theta \frac{\partial^2 \Psi}{\partial \mathbf{C} \partial \theta} = -2\theta \frac{\partial^2 \Psi}{\partial \theta \partial \mathbf{C}}, \quad \rho C = -\theta \frac{\partial^2 \Psi}{\partial \theta^2}, \quad (6)$$

where \mathbb{C} is the fourth-order isothermal elasticity tensor, $\boldsymbol{\zeta}$ is the second-order latent heat tensor at constant deformation, C is the scalar specific heat at constant deformation, and ρ is the density. Furthermore, a thermodynamic Maxwell equation can be obtained by Equating (6)₂ and (6)₃ and using (4)₁ and (4)₂

$$\left(\frac{\partial \mathbf{S}}{\partial \theta} \right)_{\mathbf{C}} = -2 \left(\frac{\partial \boldsymbol{\zeta}}{\partial \mathbf{C}} \right)_{\theta}. \quad (7)$$

The classical theories of thermoelasticity along with its isotropic linear thermoelastic implementations have been summarized by Vujanović and Lubarda (2002) [2].

The contemporary theory of thermoelasticity, on the other hand, has the constitutive model of finite thermoelastic deformation formulated with the multiplicative decomposition of the deformation gradient. With the imaginary intermediate configuration Ω_θ between the reference and current configurations, the deformation gradient decomposes into the product of purely thermal and purely mechanical deformation gradients

$$\mathbf{F} = \frac{\partial \mathbf{x}}{\partial \mathbf{X}_0} = \frac{\partial \mathbf{x}}{\partial \mathbf{X}_\theta} \frac{\partial \mathbf{X}_\theta}{\partial \mathbf{X}_0} = \mathbf{F}_m \mathbf{F}_\theta, \quad (8)$$

where \mathbf{X}_0 , \mathbf{X}_θ , and \mathbf{x} are position vectors in reference, intermediate, and current configurations, respectively shown in **Figure 1**. For general deformation and temperature fields, \mathbf{F} is the deformation gradient tensor while \mathbf{F}_m and \mathbf{F}_θ are local mechanical and thermal deformation gradient tensors. This multiplicative decomposition was introduced in finite thermoelasticity by Stojanović, Djurić, and Vujošević (1964) [3]. The mathematical foundations of intermediate configurations have been addressed by Goodbrake, Goriely, and Yavari (2021) [4].

The thermal deformation gradient tensor for isotropic materials can be specified in general as

$$\mathbf{F}_\theta = \mathcal{G}(\theta) \mathbf{I}, \quad (9)$$

where $\mathcal{G} = \mathcal{G}(\theta)$ is the thermal stretch and \mathbf{I} is the second-order unit tensor.

With the product of deformation gradients (8)₃ and the isotropic thermal deformation gradient (9), the decomposed mechanical part of right Cauchy-Green tensor is given by

$$\mathbf{C}_m = \mathbf{F}_m^T \mathbf{F}_m = (\mathbf{F} \mathbf{F}_\theta^{-1})^T (\mathbf{F} \mathbf{F}_\theta^{-1}) = \mathbf{F}_\theta^{-T} \mathbf{C} \mathbf{F}_\theta^{-1} = \mathbf{C} \mathcal{G}^{-2}, \quad (10)$$

and taking the time derivative of (10)₄ produces

$$\dot{\mathbf{C}}_m = \dot{\mathbf{C}} \mathcal{G}^{-2} - 2\mathcal{G}^{-2} \alpha(\theta) \mathbf{C} \dot{\theta} = \dot{\mathbf{C}} \mathcal{G}^{-2} - 2\alpha(\theta) \mathbf{C}_m \dot{\theta}, \quad (11)$$

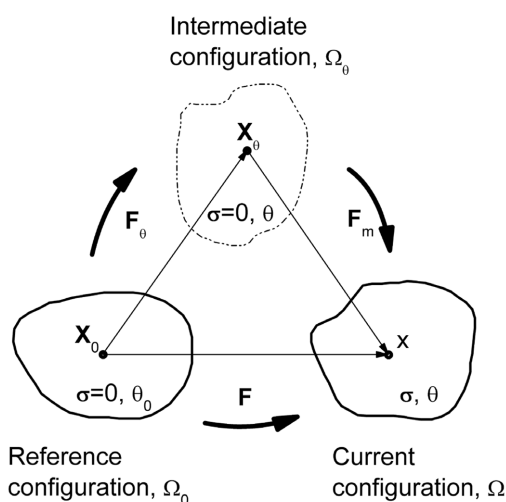


Figure 1. Multiplicative decomposition of finite thermal deformation.

in which the coefficient of thermal expansion (CTE) in stretch, $\alpha(\theta)$, is defined as

$$\alpha(\theta) = \frac{1}{\vartheta} \frac{d\vartheta}{d\theta}. \quad (12)$$

With the multiplicative decomposition of the deformation gradient, a stored energy functional can be built as

$$\Psi(C, \theta) = \vartheta^3 \Psi_m(C_m, \theta) + \Psi_\theta(\theta), \quad (13)$$

where $\Psi(C, \theta)$ is the thermal-mechanical stored energy functional per unit reference volume, $\Psi_m(C_m, \theta)$ is the mechanical stored energy functional per unit intermediate volume, and $\Psi_\theta(\theta)$ is the thermal stored energy function per unit reference volume. The additive decomposition of a stored energy functional (13) is practically applicable because $\Psi_m(C_m, \theta)$ can be selected from one of the established stored energy functionals with extended constitutive parameters as a function of temperature while $\Psi_\theta(\theta)$ can be separately determined based on the experimental test and theoretical definition of specific heat, which are reviewed by Lubarda (2004) [5].

Integrating the specific heat Equation (6)₄ gives a thermal stored energy function

$$\Psi_\theta = \rho C \left[(\theta - \theta_0) - \theta \ln \frac{\theta}{\theta_0} \right]. \quad (14)$$

For applications of the isotropic continuum stored energy (CSE) functional developed by Zhao (2016) [6], due to its advanced features, the mechanical stored energy functional can be readily formulated as

$$\Psi_m = S_m : \frac{C_m}{2}, \quad S_m = 2 \frac{\partial \Psi_m}{\partial C_m}, \quad (15)$$

Taking the time derivative of the stored energy functional (13) on the right hand side yields

$$\dot{\Psi} = \vartheta^3 2 \frac{\partial \Psi_m}{\partial C_m} : \frac{\dot{C}_m}{2} + 3\vartheta^3 \frac{1}{\vartheta} \frac{d\vartheta}{d\theta} \Psi_m \dot{\theta} + \vartheta^3 \frac{\partial \Psi_m}{\partial \theta} \dot{\theta} + \frac{d\Psi_\theta}{d\theta} \dot{\theta}, \quad (16)$$

Substituting (11)₂, (12), and (15) into (16), simplifying produces

$$\dot{\Psi} = \vartheta S_m : \frac{\dot{C}}{2} - \left[\vartheta^3 \alpha(\theta) \Psi_m - \vartheta^3 \frac{\partial \Psi_m}{\partial \theta} - \frac{d\Psi_\theta}{d\theta} \right] \dot{\theta}, \quad (17)$$

and the time derivative of the stored energy functional (13) on the left hand side, based on (2) and (4)₂, reads

$$\dot{\Psi} = S : \frac{\dot{C}}{2} - \eta \dot{\theta}, \quad S = 2 \frac{\partial \Psi}{\partial C}. \quad (18)$$

Comparing (17) to (18) gives the constitutive relations for the second Piola-Kirchhoff stress S and specific entropy η

$$S = \vartheta S_m, \quad \eta = \vartheta^3 \alpha(\theta) \Psi_m - \vartheta^3 \frac{\partial \Psi_m}{\partial \theta} - \frac{d\Psi_\theta}{d\theta}, \quad (19)$$

where the thermal stretch \mathcal{G} , as a function of temperature in general, can be obtained by integrating (12) from reference temperature θ_0 to current temperature θ as

$$\mathcal{G}(\theta) = \exp \left[\int_{\theta_0}^{\theta} \alpha(\theta) d\theta \right] = \exp [\alpha_0 (\theta - \theta_0)], \quad \text{for } \alpha(\theta) = \alpha_0. \quad (20)$$

Products made of rubberlike materials are often used in working environments under a wide range of temperatures. Environmental temperature changes can cause significant variations in mechanical properties of rubbers. Therefore, external temperature effects on mechanical properties of rubbers must be considered in their analyses and design. The Gough-Joule effect or the internal temperature effect is interesting to study because a stretched piece of rubber due to self-heating will shrink rather than expand and this very effect should be quantified and considered in design. The strain-induced crystallization (SIC) is believed to be the physical origin of mechanical hysteresis for unfilled rubberlike materials under cyclic loading. Although external, internal, and SIC related temperature effects on mechanical properties are well recognized and studied, few thermal-mechanical models attempt to quantify the stress-stretch-temperature relation, and consistent sets of experimental data including structural, calorimetric, and crystallinity characterizations of rubberlike materials are scanty (see Rodas *et al.* (2015) [7]).

The major objectives, therefore, are to extend the CSE functional to constitutively model and predict finite thermoelastic deformations of rubberlike materials. The isomorphism CSE finite thermoelastic constitutive model fits tested and predicts tested but unfitted experimental data of silicone rubber (SR) and natural rubber filled with 60 phr carbon black (NR-C60) rubbers at various external temperatures. For internal temperature effects, the CSE finite thermoelastic model, along with the newly developed CTE and crystallinity index (CI) models, fits both nominal stress-stretch and temperature change-stretch experimental data for both NR and NR-SIC rubbers.

This paper is organized as follows. In Section 2, the isomorphism CSE functional is applied for constitutive modeling finite thermoelastic deformations of rubbers due to external thermal effect, internal thermal effect, and strain-induced crystallization effect. In Section 3, the isomorphism CSE constitutive model is applied to fits uniaxial extension test data for materials with external thermal, internal thermal, and strain-induced crystallization effects. In Section 4, the theory and application details of the isomorphism CSE functional and related models are discussed. In Section 5, conclusions are drawn.

2. Isomorphism CSE Finite Thermoelastic Model

2.1. External Thermal Effect

For external thermal effects, the multiplicative decomposition of the deformation gradient is used. The isotropic CSE functional under isothermal condition has further been developed by Zhao (2020, 2021) [8] [9]

$$\Psi(\mathbf{C}) = c_1 I_1 + c_2 \sqrt{I_2} + c_3 \frac{I_1^{3c_4+1}}{I_3^{c_4}}. \quad (21)$$

The three invariants of the right Cauchy-Green tensor are defined and $\mathbf{C} = \mathbf{C}_m \cdot \mathcal{G}^2 \mathbf{I}$ (10)₄ is applied as

$$I_1 = \text{tr} \mathbf{C} = I_{m1} \mathcal{G}^2, I_2 = \frac{1}{2} \left[(\text{tr} \mathbf{C})^2 - \text{tr} \mathbf{C}^2 \right] = I_{m2} \mathcal{G}^4, I_3 = \det \mathbf{C} = I_{m3} \mathcal{G}^6, \quad (22)$$

where the three invariants of \mathbf{C}_m are defined and utilized by Lu and Pister (1975) [10]

$$I_{m1} = \text{tr} \mathbf{C}_m, I_{m2} = \frac{1}{2} \left[(\text{tr} \mathbf{C}_m)^2 - \text{tr} \mathbf{C}_m^2 \right], I_{m3} = \det \mathbf{C}_m, \quad (23)$$

Substituting $\mathbf{C} = \mathbf{C}_m \cdot \mathcal{G}^2 \mathbf{I}$, (22), and (23) into (21) yields

$$\begin{aligned} \Psi(\mathbf{C}) &= \Psi(\mathbf{C}_m \cdot \mathcal{G}^2 \mathbf{I}) = \left(c_1 I_{m1} + c_2 \sqrt{I_{m2}} + c_3 \frac{I_{m1}^{3c_4+1}}{I_{m3}^{c_4}} \right) \mathcal{G}^2 \\ &= \Psi(\mathbf{C}_m) \cdot \Psi(\mathcal{G}^2 \mathbf{I}) = \Psi(\mathbf{C}_m) \mathcal{G}^2. \end{aligned} \quad (24)$$

For the bijective mapping $\Psi: G \rightarrow G'$, the multiplication operation, $\Psi(\mathbf{C}_m \cdot \mathcal{G}^2 \mathbf{I}) = \Psi(\mathbf{C}_m) \cdot \Psi(\mathcal{G}^2 \mathbf{I})$, is preserved. Thus, the isotropic CSE functional, Ψ , is an isomorphism group with domain G and range G' . The finite thermoelastic CSE functional is related to the total CSE functional (21) due to different configurations by

$$\Psi(\mathbf{C}) = \mathcal{G}^3 \Psi_m(\mathbf{C}_m, \theta) = \mathcal{G}^3 \left(c_{\theta 1} I_{m1} + c_{\theta 2} \sqrt{I_{m2}} + c_{\theta 3} \frac{I_{m1}^{3c_{\theta 4}+1}}{I_{m3}^{c_{\theta 4}}} \right). \quad (25)$$

Comparing constitutive parameters between (24)₂ and (25)₂ generates the following relation

$$c_{\theta i} = c_i \mathcal{G}^{-1}, (i = 1, 2, 3) \text{ and } c_{\theta 4} = c_4. \quad (26)$$

The finite thermoelastic CSE functional with the preserved structure of symmetry in Ψ reads

$$\Psi_m(\mathbf{C}_m, \theta) = \left(c_1 I_{m1} + c_2 \sqrt{I_{m2}} + c_3 \frac{I_{m1}^{3c_4+1}}{I_{m3}^{c_4}} \right) \mathcal{G}^{-1}, \quad (27)$$

where the four constitutive parameters, c_1 , c_2 , c_3 , and c_4 , will then be determined by experimental tests at reference temperature θ_0 . Thus, the finite thermoelastic CSE functional (27) will be used to establish constitutive model for uniaxial extension tests at various external temperatures.

Nominal stress and stretch results are preferably calculated from force and extension measurements with original sample dimensions recorded in experimental tests. The nominal stress as a function of stretch in indicial notation reads

$$P_{m,ji} = \frac{\partial \Psi_m}{\partial I_{m1}} \frac{\partial I_{m1}}{\partial \Lambda_{ij}} + \frac{\partial \Psi_m}{\partial I_{m2}} \frac{\partial I_{m2}}{\partial \Lambda_{ij}} + \frac{\partial \Psi_m}{\partial I_{m3}} \frac{\partial I_{m3}}{\partial \Lambda_{ij}}, (i, j = 1, 2, 3). \quad (28)$$

The three derivatives of the CSE finite thermoelastic functional (27) for rub-

ber-like materials with the incompressible assumption are

$$\frac{\partial \Psi_m}{\partial I_{m1}} = [c_1 + c_3(3c_4 + 1)I_{m1}^{3c_4}]g^{-1}, \frac{\partial \Psi_m}{\partial I_{m2}} = \frac{c_2}{2\sqrt{I_{m2}}}g^{-1}, \frac{\partial \Psi_m}{\partial I_{m3}} = 0. \quad (29)$$

In uniaxial extension tests, the three mechanically equivalent invariants are given by

$$I_{m1} = \Lambda^2 + 2\Lambda^{-1}, \quad I_{m2} = 2\Lambda + \Lambda^{-2}, \quad I_{m3} = 1, \quad (30)$$

and the derivatives of mechanical invariants with respect to Λ are

$$\frac{\partial I_{m1}}{\partial \Lambda} = 2\Lambda - 2\Lambda^{-2}, \quad \frac{\partial I_{m2}}{\partial \Lambda} = 2 - 2\Lambda^{-3}, \quad \frac{\partial I_{m3}}{\partial \Lambda} = 0. \quad (31)$$

Substituting (29), (30), and (31) into (28) and using (20)₂ yields

$$P_m = \left[2c_1(\Lambda - \Lambda^{-2}) + c_2(1 - \Lambda^{-3}) \right] / \sqrt{2\Lambda + \Lambda^{-2}} + 2c_3(3c_4 + 1)(\Lambda^2 + 2\Lambda^{-1})^{3c_4}(\Lambda - \Lambda^{-2}) \exp[-\alpha_0(\theta - \theta_0)]. \quad (32)$$

where the nominal stress in uniaxial extension mode P_m as a function of mechanical stretch $\Lambda = \lambda/g$ and temperature θ in (32) can be used to model mechanical responses of incompressible isotropic hyperelastic materials at different environmental temperatures.

2.2. Internal Thermal Effect

The strain-induced thermal effect or the internal thermal effect on rubberlike materials is formulated based on the isotropic CSE functional originally developed for modeling nonlinear elastic deformation under isothermal processes. For coupled finite thermoelastic deformations with incompressible assumption, using the method of variation of the constants, the isothermal CSE functional can be extended by converting constant constitutive parameters into variables and combined with (14) as,

$$\Psi(C, \theta) = c_{\theta 1}(I_1 - 3) + c_{\theta 2}(\sqrt{I_2} - \sqrt{3}) + c_{\theta 3}(I_1^{3c_{\theta 4}+1} - 3^{3c_{\theta 4}+1}) + \rho C \left[(\theta - \theta_0) - \theta \ln \frac{\theta}{\theta_0} \right]. \quad (33)$$

Substituting (26) into (33) gives

$$\Psi(C, \theta) = \left[c_1(I_1 - 3) + c_2(\sqrt{I_2} - \sqrt{3}) + c_3(I_1^{3c_4+1} - 3^{3c_4+1}) \right] g^{-1} + \rho C \left[(\theta - \theta_0) - \theta \ln \frac{\theta}{\theta_0} \right], \quad (34)$$

where the isothermal constitutive parameters c_1, c_2, c_3 , and c_4 can be determined by the coupled thermal-mechanical experimental stress with the internal thermal effect removed as

$$P_{e0} = P_e \exp[\alpha_d(\theta - \theta_0)] \approx P_e [1 + \alpha_d(\theta - \theta_0)], \quad \text{for } \alpha_d(\theta - \theta_0) \ll 1, \quad (35)$$

where P_{e0} is the isothermally converted experimental nominal stress and P_e

is the original experimental nominal stress. The nominal stress with the internal thermal effect using (34) turns out to be

$$P(\lambda, \theta) = P_0 \exp[-\alpha_d(\theta - \theta_0)] \approx P_0/[1 + \alpha_d(\theta - \theta_0)], \text{ for } \alpha_d(\theta - \theta_0) \ll 1, \quad (36)$$

where the isothermal nominal stress P_0 in uniaxial extension mode is

$$P_0 = 2(\lambda - \lambda^{-2})c_1 + \frac{1 - \lambda^{-3}}{\sqrt{2\lambda + \lambda^{-2}}}c_2 + 2(3c_4 + 1)(\lambda^2 + 2\lambda^{-1})^{3c_4}(\lambda - \lambda^{-2})c_3. \quad (37)$$

For coupled finite thermoelastic deformations, the CTE as a function of temperature, $\alpha(\theta)$, can be converted as a function of stretch $\lambda = L/L_0$. A new CTE model can then be defined and derived with both initial and current lengths treated as function of temperature, in which the same treatment has also been used by Pellicer *et al.* (2001) [11]

$$\alpha(\theta) = \frac{1}{\lambda} \frac{d\lambda}{d\theta} = \frac{1}{L} \frac{dL}{d\theta} - \frac{1}{L_0} \frac{dL_0}{d\theta} = \alpha_d - \alpha_{d0}. \quad (38)$$

Integrating (38)₁, (38)₃, equating both integration results, and rearranging yields

$$\alpha_d(\lambda) = \alpha_{d0} + c_\alpha \ln \lambda, \quad (39)$$

where c_α is a parameter of the CTE model (39) to be determined by experimental tests.

The converted experimental data by (35) will be used to fit the isothermal nominal stress (37). Once the isothermal constitutive parameters, c_1, c_2, c_3 , and c_4 , are determined, the temperature profile may be modeled by the entropy constitutive model

$$\eta = \alpha_d \left[c_1(I_1 - 3) + c_2(\sqrt{I_2} - \sqrt{3}) + c_3(I_1^{3c_4+1} - 3^{3c_4+1}) \right] \exp[-\alpha_d(\theta - \theta_0)] + \rho C \ln \left(\frac{\theta}{\theta_0} \right). \quad (40)$$

For $\alpha_d(\theta - \theta_0) \ll 1$, the entropy constitutive model (40) for temperature change can be simplified as

$$\Delta\theta = \theta - \theta_0 = -\Psi_0(\lambda) \frac{\alpha_d \theta_0}{\rho C} + \frac{\eta \theta_0}{\rho C}, \quad (41)$$

where the isothermal CSE function, $\Psi_0(\lambda)$, in uniaxial extension mode with the incompressible assumption is given by

$$\Psi_0(\lambda) = c_1(\lambda^2 + 2\lambda^{-1} - 3) + c_2(\sqrt{2\lambda + \lambda^{-2}} - \sqrt{3}) + c_3 \left[(\lambda^2 + 2\lambda^{-1})^{3c_4+1} - 3^{3c_4+1} \right]. \quad (42)$$

2.3. Strain-Induced Crystallization Effect

For crystallizable rubberlike materials, the SIC effect on both stress and temperature change need to be considered. The CSE functional can be augmented as

$$\Psi = \frac{c_1(I_1 - 3) + c_2(\sqrt{I_2} - \sqrt{3}) + c_3(I_1^{3c_4+1} - 3^{3c_4+1})}{1 + \alpha_d(\theta - \theta_0)} + \Psi_\theta + \Psi_\chi, \quad (43)$$

where the isothermal constitutive parameters c_1, c_2, c_3 , and c_4 can be determined by the coupled thermal-mechanical-crystallization experimental stress with both internal thermal and SIC effects removed

$$P_{e0\chi} = P_e [1 + \alpha_d(\theta - \theta_0)] + c_{\chi p} \chi(\lambda). \quad (44)$$

where $P_{e0\chi}$ is the converted experimental isothermal nominal stress without both internal thermal and SIC effects and P_e is the original experimental nominal stress. The crystallinity index (CI) model is defined as

$$\chi(\lambda) = \begin{cases} c_{\chi 1} \left\{ 1 - \exp \left[-c_{\chi 2} (\lambda - \lambda_{c1})^2 \right] \right\}, & \lambda_{c1} \leq \lambda \leq \lambda_{c2}, \\ 0, & \text{otherwise.} \end{cases} \quad (45)$$

where $c_{\chi 1}$ and $c_{\chi 2}$ are two parameters of the CI model to be fixed by experimental tests. Two critical stretches, λ_{c1} and λ_{c2} , define the start and end of SIC during loading and the end and start of decrystallization during unloading, respectively. The actual nominal stress as a function of stretch, temperature, and crystallinity can then be modeled as

$$P(\lambda, \theta, \chi) = [P_0 - c_{p\chi} \chi(\lambda)] / [1 + \alpha_d(\theta - \theta_0)], \quad (46)$$

and the temperature change can be modeled by

$$\Delta\theta = \theta - \theta_0 = -\Psi_0(\lambda) \alpha_d(\lambda) c_c + c_\eta + c_{\chi\theta} \chi(\lambda), \quad (47)$$

where $c_c = \theta_0 / \rho C$, c_η , $c_{p\chi}$, and $c_{\chi\theta}$ are model parameters corresponding to heat capacity, entropy, SIC effect on stress, and SIC effect on temperature change, respectively.

3. Applications of CSE Finite Thermoelastic Model

3.1. External Thermal Effect on Unfilled Silicone Rubbers

Silicone rubbers (SR) have many applications in the automotive, food storage product, footwear, electronics, and medical device industries. Modeling their mechanical responses at various temperatures are needed in product design and analyses. The uniaxial extension tests of both unfilled and filled SR rubbers have been conducted at different temperatures with the stretch rate of 1.67 s^{-1} by Rey *et al.* (2013) [12]. The nominal stress-stretch experimental data in loading of unfilled SR rubbers at temperatures of 293 K, 333 K, 373 K, and 423 K has been selected among others. A self-developed graphics digitizer with MATLAB has been used to read out all the related experimental data. Stresses at certain stretches increase with temperatures which highlight the entropic behavior of the unfilled silicone rubber for temperatures way above the crystallization temperature of 190 K. The constitutive parameters of the CSE finite thermoelastic constitutive Equation (32) have numerically been solved and fitted for the uniaxial extension test at $\theta = 293 \text{ K}$. The obtained constitutive parameters and $\theta = 423 \text{ K}$ have

been submitted into (32) to determine α_0 through the best-fit between the CSE model and the test data at $\theta = 423$ K. Once all constitutive parameters are determined, the nominal stress-stretch relations at 333 K and 373 K have been predicted, respectively. The comparison between the CSE model and the experimental data is shown in **Figure 2**. The thermal and mechanical constitutive parameters are listed in **Table 1**.

3.2. External Thermal Effect on Filled Natural Rubbers

Uniaxial extension tests of carbon black filled natural rubbers at different temperatures have been conducted by Fu *et al.* [13]. Ten cycles of cyclic stretching have been conducted to remove the Mullins effect before monotonic tests. The nominal stress-stretch test results for vulcanized natural rubber filled with 60 phr carbon black (NR-C60) at the temperatures of 293 K, 313 K, and 333 K have been selected for constitutive modeling and predicting. Stress-decreasing effects have been observed as external testing temperature increases. The constitutive parameters of the CSE finite thermoelastic constitutive equation in uniaxial

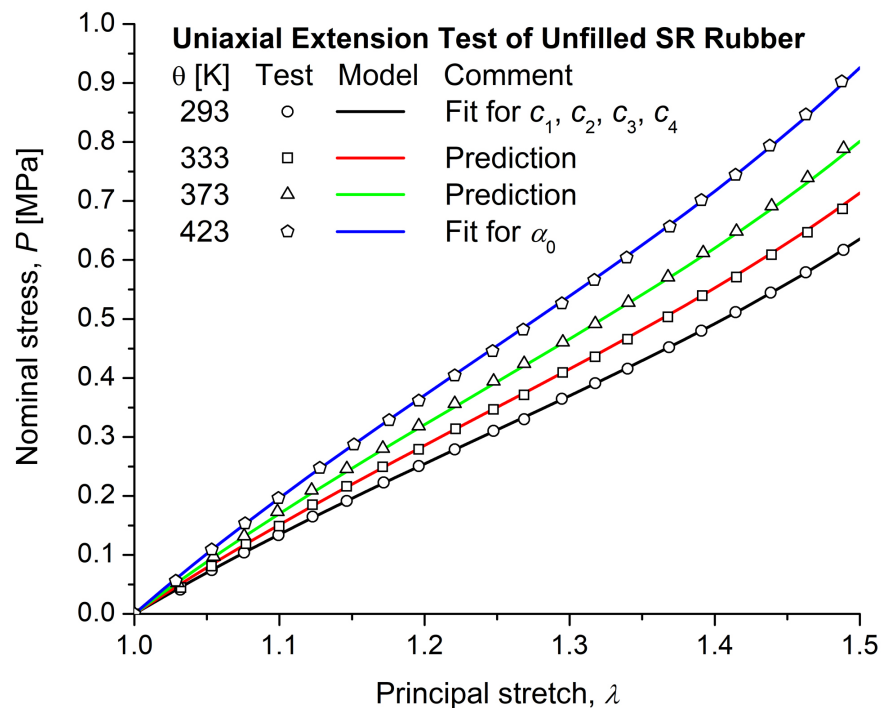


Figure 2. Comparison between test and model for unfilled SR rubber.

Table 1. Constitutive parameters of the CSE model with external thermal effects.

Material	c_1 (MPa)	c_2 (MPa)	c_3 (MPa)	c_4	α_0 (1/K)
SR Rubber	0.2230	-0.0146	2.97×10^{-6}	2.1427	-0.0029
NR-C60 Rubber	0.5583	1.1284	2.48×10^{-5}	1.5778	0.0095

extension mode (32) at $\theta_0 = 293$ K have been determined. The constitutive parameters and $\theta = 333$ K have been submitted into (32) to determine α_0 based on the minimization of a percentage error. With all determined constitutive parameters, the nominal stress-stretch relation at 313 K has been predicted. The comparison between the CSE model and the experimental data is shown in **Figure 3**. The thermal and mechanical constitutive parameters are also listed in **Table 1**.

3.3. Internal Thermal Effect of NR Rubber

Coupled with thermomechanical responses, the Gough-Joule effect of vulcanized natural rubber (NR) under uniaxial extension till rupture tests have been studied at room temperature with the stretch rate of 5 s^{-1} by Staszczak *et al.* (2015) [14]. A self-developed graphics digitizer with MATLAB has been used to read out all the related experimental data. The true stress and true strain data have been converted to nominal stress and stretch data, respectively. The CTE model (39) fits Joule's six experimental data [15] and one key data at the thermoelastic inversion point of $\alpha_d(\lambda_{\text{inv}}) = 0$, at which the maximum temperature drop occurs (see Price (1976) [16]). The constitutive parameters of the isothermal CSE model (37) for converted test data by $(35)_2$ have been determined and the CSE finite thermoelastic model $(36)_2$ and the entropy CSE model (41) along with (42) for the original test data of both stress and temperature change against principal stretch are plotted and compared in **Figure 4(a)**. The comparison between the CTE model and the Joule's experimental data of crosslinked NR rubbers is shown in **Figure 4(b)**. The brief thermal and mechanical constitutive parameters

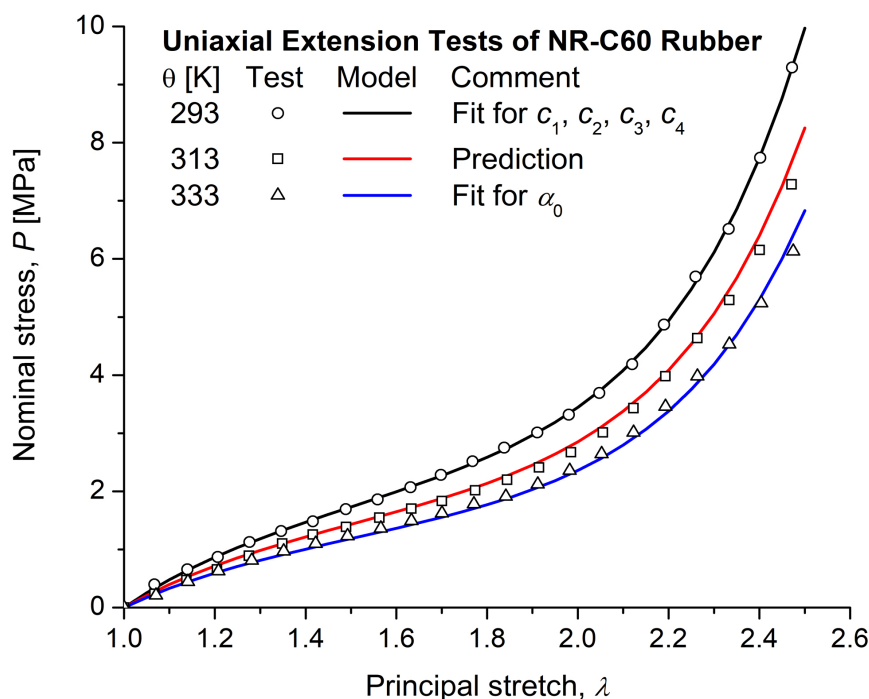


Figure 3. Comparison between test and model for filled NR-C60 rubber.

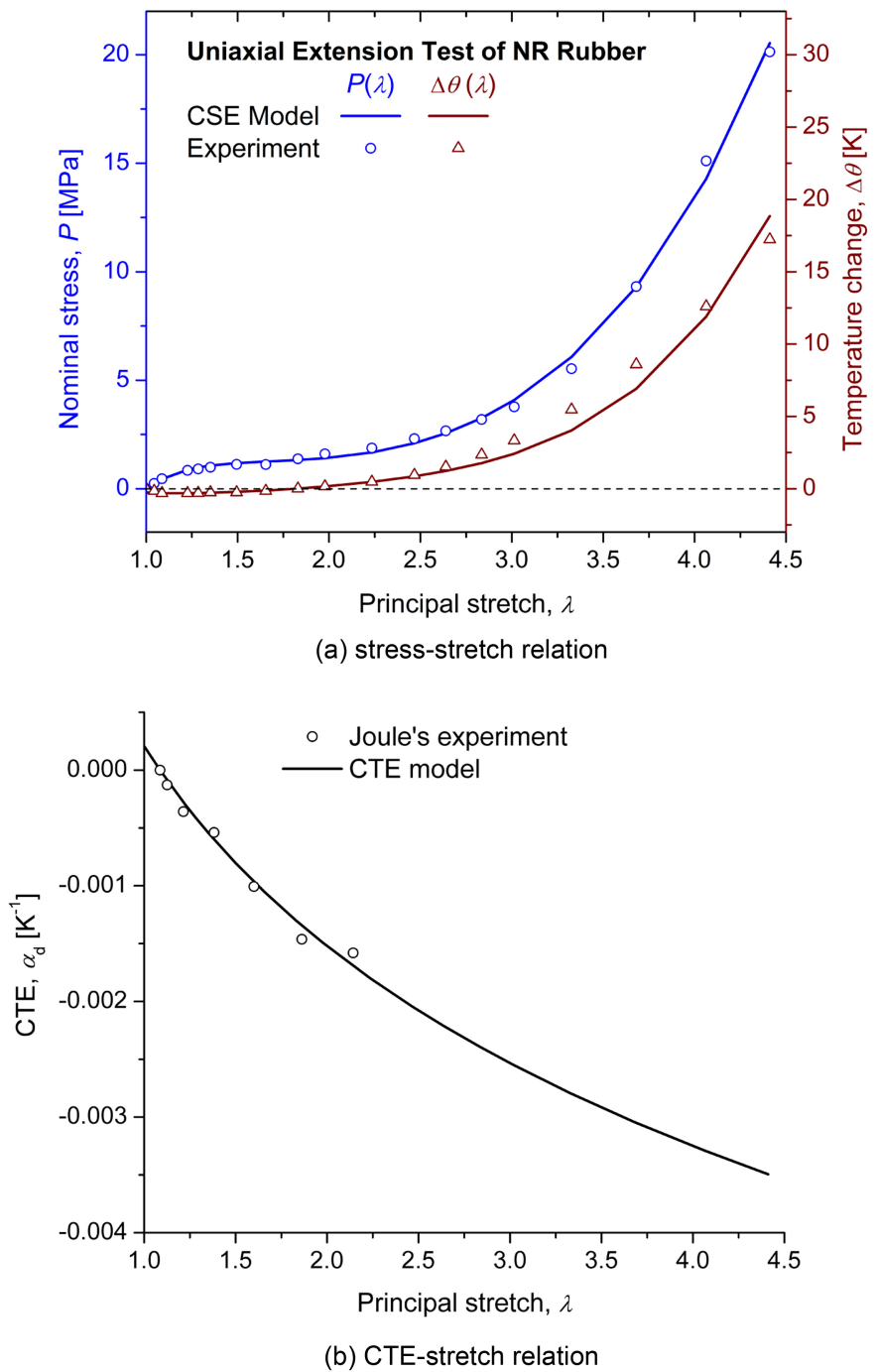


Figure 4. Comparison of stress and temperature change between test and model for NR rubber.

are listed in **Table 2**.

3.4. SIC and Thermal Effects on NR Rubber

Thermal and SIC effects on crosslinked NR rubber in cyclic uniaxial extension tests have been studied at room temperature with the stretch rate of $\pm 0.5/s$ by Samaca Martinez *et al.* (2013) [17]. A self-developed graphics digitizer with

Table 2. Constitutive parameters of the CSE model with internal thermal effects.

Material	c_1 (MPa)	c_2 (MPa)	c_3 (MPa)	c_4	α_{d0} (1/K)	c_α (1/K)
NR	-0.5179	4.8704	1.26×10^{-02}	0.4906	0.0002	-0.0025
NR-SIC	0.2624	0.2434	1.13×10^{-05}	0.7678	0.0000	-0.0025
NR-SIC	0.3131	-0.3017	5.21×10^{-11}	1.8084	0.0000	-0.0025

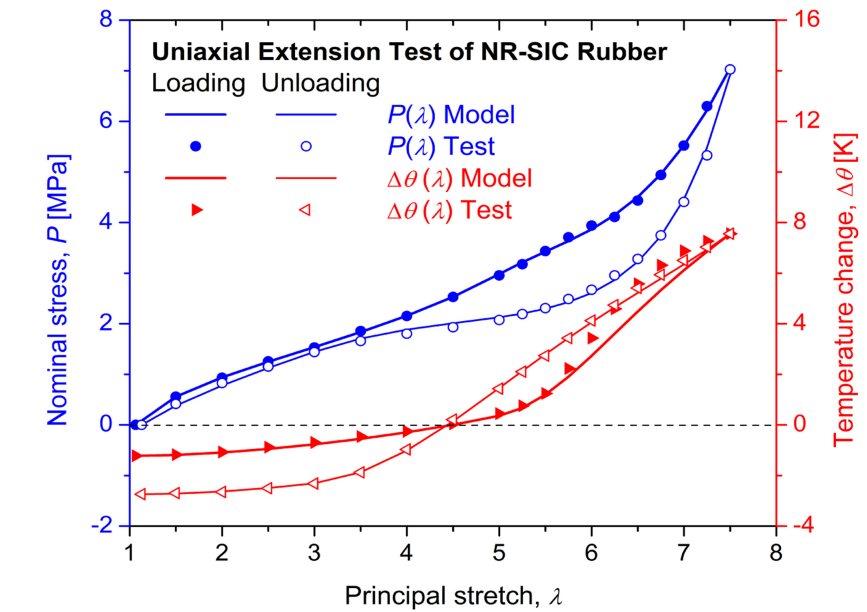
MATLAB has been used to read out the nominal stress coupled with temperature change experimental data as functions of stretch at the tenth cycle of loading and unloading. The experimental data of crystallinity index against stretch published by Le Cam (2018) [18] has also been obtained. The constitutive parameters of the isothermal CSE model (37) for converted test data by (44) have been determined and the thermal-mechanical-crystallization CSE model (46) and the corresponding entropy CSE model (47) along with (42) for the original test data of both stress and temperature change against principal stretch have been compared and plotted in **Figure 5(a)**. The CI model (45) fits the experimental CI data and the comparison of CI between model and test is shown in **Figure 5(b)**. The thermal, mechanical, and SIC constitutive parameters are also listed in **Table 2**.

4. Discussion

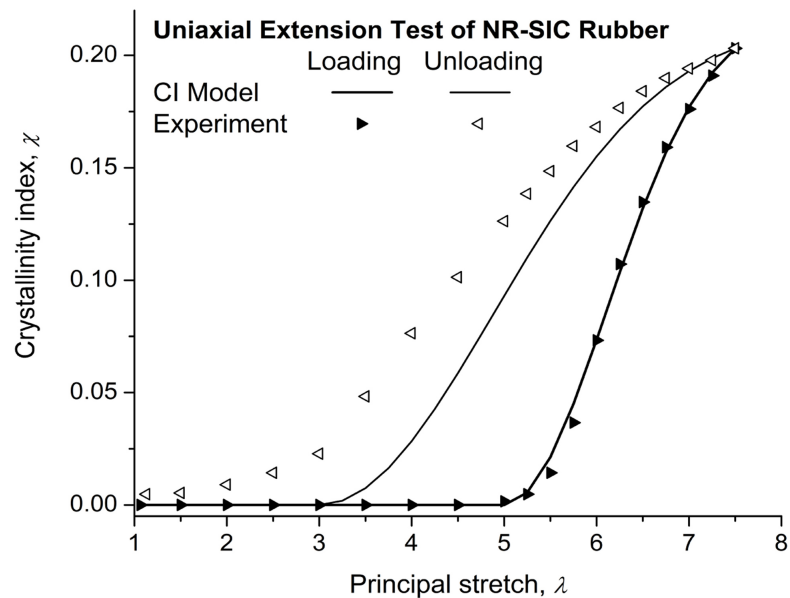
4.1. Isomorphism CSE Functional

The commonly used measures for hyperelastic deformations are \mathbf{F} , \mathbf{C} , and \mathbf{E} . The right Cauchy-Green tensor $\mathbf{C} = \mathbf{F}^T \mathbf{F}$ cancels out possible rigid body rotations in \mathbf{F} . The Green-Lagrange strain tensor, $\mathbf{E} = 0.5(\mathbf{C} - \mathbf{I})$, could create singularities and imaginary numbers in constitutive modelings as studied by Zhao (2016) [6]. Furthermore, stress-stretch curves of hyperelastic materials are strictly increasing functions, which are injective. Additionally, every stress on the curve must be corresponding to at least one stretch, which requires a surjective function. A function that is both injective and surjective is called a bijective function in terms of abstract algebra as documented by Pinter (1990) [19]. For constructing a bijective functional, the stretch-based tensor \mathbf{C} rather than the strain tensor \mathbf{E} is used since stretch, $\lambda \in \mathbb{R}^+$, is always a positive real number.

The partial differential equation of the isotropic CSE functional is covariantly formulated by the stretch-based stress work done, generally resolved by the Lie group method, and particularly determined by differential geometry. The three terms of the isotropic CSE functional (21) possess the same order of magnitude, λ^2 , since they are asymptotically equal, representing normal stretch, shear stretch, and ellipsoidal stretch deformations. This unique feature of the CSE functional, not possessed in other full functionals with three invariants I_1 , I_2 , and I_3 , makes Ψ an isomorphism under the multiplication $\Psi(\mathbf{C}_m \cdot \mathcal{I}^2 \mathbf{I}) = \Psi(\mathbf{C}_m) \cdot \Psi(\mathcal{I}^2 \mathbf{I})$. Therefore, the finite thermoelastic CSE functional (27) preserves the structure of symmetry in Ψ (21). Indeed, thermal



(a) stress-stretch relation



(b) CI-stretch, relation

Figure 5. Comparison of SIC effects between test and model for NR-SIC rubber.

deformation does not affect the form of the hyperelastic constitutive relation, which was one kind of material isomorphism assumed by Noll (1972) [20]. The concept of material isomorphism was later applied to finite elastoplasticity formulations by Svendsen (1998) [21] and Bertram (1999) [22] among others.

4.2. External Thermal Effect

For modeling external thermal effects on mechanical response of rubberlike ma-

materials such as stress-stretch relations at different temperatures, the multiplicative decomposition of deformation gradient (8) has been widely used. Furthermore, the thermal effect is clearly and cleanly captured as the product of \mathcal{G}^{-1} on isothermal mechanical behaviors. Mathematically, the advanced feature of the CSE functional with the relation of constitutive parameters (26) equally weights thermal effects on all dimensional constitutive parameters $c_{\theta 1} = c_1 \mathcal{G}^{-1}$, $c_{\theta 2} = c_2 \mathcal{G}^{-1}$, $c_{\theta 3} = c_3 \mathcal{G}^{-1}$, but no change occurs on the dimensionless constitutive parameter since $c_{\theta 4} = c_4$. Physically, the isotropic thermal effect equally weights and imposes on the normal stretch, shear stretch, and ellipsoidal stretch deformations of the CSE functional.

As we have known, CTEs with respect to distance, area, and volume have already been defined and widely utilized. In geometry, distance is the most basic measure among distance, area, and volume since distance can be readily used to express area and volume but generally not the other way around. In other words, higher dimension measures result in more hidden or lost information. Therefore, the coefficient of thermal expansion in distance is used extensively.

In curve-fitting both SR and NR-C60 cases, isothermal constitutive parameters are determined at room temperature of $\theta_0 = 293$ K. The negative CTE value for the SR case, corresponding to thermal contraction, is then fixed by refitting the nominal stress-stretch testing data at $\theta = 423$ K while the positive CTE value for NR-C60 case, corresponding to thermal expansion, is obtained by refitting nominal stress-stretch testing data at $\theta = 333$ K albeit other available options. The predictions of nominal stress-stretch relations within the studied range of temperature can be confidently made and some comparisons of both SR and NR-C60 rubbers have shown in **Figure 2** and **Figure 3**, respectively.

4.3. Internal Thermal Effect

In modeling self-heating effects, the CTE model $\alpha_d(\lambda)$ expressed in (39) is desired. Stresses at the thermoelastic inversion stretch are not influenced by temperatures so that the CTE value at the inversion point must be zero (see Anthony, Caston, and Guth (1942) [23]). The CTE model has been fitted with the condition of $\alpha_d(\lambda_{\text{inv}}) = 0$ along with Joule's six experimental data. The rearranged CTE model, $\alpha_d = c_\alpha \ln(\lambda/\lambda_{\text{inv}})$, is actually fitted with Joule's data shown in **Figure 4(b)**. In the NR case with $\lambda_{\text{inv}} = 1.08670$, the parameter of CTE model is obtained as $c_\alpha = -0.0024944$ [1/K]. The CTE value for crosslinked NR rubber at no deformation is predicted as $\alpha_{d0} = 0.0002074$ [1/K], which is very closed to the value of 0.0002233 [1/K] documented in [24].

In modeling self-heating effects, the entropy constitutive model (41) is used to fit temperature change experimental data. In the first term, the specific heat ρC , along with constant temperature θ_0 , is tacitly treated as a lumped constant c_c although it changes slightly within the practical temperature gamut for stretched NR rubbers. For curve fitting, a best fit occurs at $c_c = 311$ [K²/MPa]. The zero temperature change condition at no deformation of $\Delta\theta|_{\lambda=1} = 0$ and

the thermoelastic inversion condition of $\alpha_d(\lambda_{\text{inv}}) = 0$ require the entropy term to be a variable. To satisfy both conditions mentioned above, the second term is simply treated as a piecewise function

$$\frac{\eta\theta_0}{\rho C} = \begin{cases} \Delta\theta_{\min}(\lambda-1)/(\lambda_{\text{inv}}-1), & 1 \leq \lambda \leq \lambda_{\text{inv}}, \\ \Delta\theta_{\min}, & \text{otherwise.} \end{cases} \quad (48)$$

In Equation (48), $\Delta\theta_{\min}$ is the minimum value of temperature change. The comparison between test data and model fits for both nominal stress and temperature change against principal stretch have been shown in **Figure 4**. The self-heating effects on finite deformation of NR rubbers has been studied with the combined efforts of CTE test data by Joule (1859) [15], the thermoelastic inversion condition mentioned by Price (1976) [16], the stress-stretch, and the temperature change-stretch experimental data by Staszczak *et al.* in 2015 [14]. In practical finite element analyses of product designs using rubberlike materials, isothermal constitutive models are usually used to fit experimental tests embedded with the self-heating effect. This study also confirms that the internal thermal effect on mechanical responses of rubberlike materials can indeed be ignored due to their thermal properties of $\alpha_d\Delta\theta \ll 1$ albeit a little impact on mechanical responses of rubbers at finite stretches.

4.4. Strain-Induced Crystallization Effect

The SIC effect is well believed to be the physical origin of mechanical hysteresis for unfilled rubberlike materials under cyclic loading. The modeling of mechanical and calorimetric responses of NR-SIC under cyclic loading is similar to that of NR under monotonic loading. The difference is that $\alpha_{d0} = 0$ is assumed for the cyclic loading NR-SIC case. The entropy term is treated as a constant with $c_\eta = \Delta\theta_{\min}$ so that isentropic thermodynamic processes are assumed in the curve fitting of temperature change model (47).

For curve-fitting the CI model (45), rather than other available models by Candau *et al.* (2012) [25] and Loos *et al.* (2021) [26], the best fit of loading CI data and the best fit of temperature change on unloading CI data have been conducted and the results have been shown in **Figure 5(b)**. The over melting or over decrystallization in CI experimental data in the twelfth cycle is removed. The comparison of both stress and temperature change against principal stretch between tests and models has been shown in **Figure 5**. The important parameters related to the CI model are listed in **Table 3**.

The area change of the mechanical hysteresis loop was not observed between the two stretch rates of 0.5 s^{-1} for structural and calorimetric characterizations

Table 3. Parameters related to CI model for NR-SIC rubber.

Cycle-Type	c_{x1}	c_{x2}	λ_{c1}	λ_{c2}	$c_{xp} [\text{MPa}]$	$c_{x\theta} [\text{K}]$
Loading	0.2207	0.4052	5.0	7.5	6.0000	19.7004
Unloading	0.2155	0.1413	3.0	7.5	6.0000	27.7619

and $1/6 \text{ s}^{-1}$ for the CI characterization. Thus, the effects of thermal dissipation due to viscous heating on the hysteresis loop are negligible as emphasized by Le Cam [27]. Little difference on the experimental nominal stress-stretch curves between the tenth cycle and the twelfth cycle appears while large difference on the experimental temperature change-stretch curves between the tenth cycle and the twelfth cycle can be seen due to heat accumulation.

5. Conclusions

Mechanical responses of rubberlike materials are mainly impacted by external thermal, internal thermal, and SIC effects. The isomorphism CSE functional is extended to model and predict finite thermoelastic responses for rubberlike materials while preserving the structure of symmetry for finite structural deformations.

The multiplicative decomposition of deformation gradient similarly decomposes the scalar CSE functional, the second-order stress tensor, and the fourth-order elasticity tensor. The thermal effect is captured as the product of \mathcal{S}^{-1} with isothermal quantities such as the CSE functional and derived stresses. The same thermal effect on mechanical responses of normal strength c_1 , shear strength c_2 , ellipsoidal strength c_3 but little influence on the degree of chain alignment c_4 is uniquely determined for the CSE model. The isomorphism CSE finite thermoelastic model accurately fits and predicts the external thermal effects on mechanical responses of uniaxial extension for SR and NR-C60 rubbers.

The Gough-Joule effect can be modeled within the frame of two configurations by using isothermal CSE model to fit experimental data with the internal thermal effect removed. The coupled effect is then modeled with the isothermally determined constitutive parameters with the internal thermal effect recovered on model. The isotropic CSE model with the internal thermal effect, along with the CTE model and the CI model, fits the uniaxial extension tests for NR and NR-SIC rubbers.

Acknowledgements

The author is immensely grateful to Jianming and Jiesi Zhao for their support, encouragement, and assistance.

Conflicts of Interest

The author declares no conflicts of interest regarding the publication of this paper.

References

- [1] Holzapfel, G.A. and Simo, J.C. (1996) Entropy Elasticity of Isotropic Rubber-Like Solids at Finite Strains. *Computer Methods in Applied Mechanics and Engineering*, **132**, 17-44. [https://doi.org/10.1016/0045-7825\(96\)01001-8](https://doi.org/10.1016/0045-7825(96)01001-8)
- [2] Vujošević, L. and Lubarda, V.A. (2002) Finite-Strain Thermoelasticity Based on

- Multiplicative Decomposition of Deformation Gradient. *Theoretical and Applied Mechanics*, **28-29**, 379-399. <https://doi.org/10.2298/TAM0229379V>
- [3] Stojanović, R., Djurić, S., and Vujošević, L. (1964) On Finite Thermal Deformations. *Archiwum Mechaniki Stosowanej*, **1**, 103-108.
 - [4] Goodbrake, C., Goriely, A. and Yavari, A. (2021) The Mathematical Foundations of Anelasticity: Existence of Smooth Global Intermediate Configurations. *The Royal Society*, **477**, Article 20200462. <https://doi.org/10.1098/rspa.2020.0462>
 - [5] Lubarda, V.A. (2004) Constitutive Theories Based on the Multiplicative Decomposition of Deformation Gradient: Thermoelasticity, Elastoplasticity, and Biomechanics. *Applied Mechanics Reviews*, **57**, 95-108. <https://doi.org/10.1115/1.1591000>
 - [6] Zhao, F.Z. (2016) Continuum Constitutive Modeling for Isotropic Hyperelastic Materials, *Advances in Pure Mathematics*, **6**, 571-582. <https://doi.org/10.4236/apm.2016.69046>
 - [7] Rodas, C.O., Zaïri, F., Naït-Abdelaziz, M. and Charrier, P. (2015) Temperature and Filler Effects on the Relaxed Response of Filled Rubbers: Experimental Observations on a Carbon-Filled SBR and Constitutive Modeling. *International Journal of Solids and Structures*, **58**, 309-321. <https://doi.org/10.1016/j.ijsolstr.2014.11.001>
 - [8] Zhao, F.Z. (2020) Modeling and Implementing Compressible Isotropic Finite Deformation without the Isochoric—Volumetric Split. *Journal of Advances in Applied Mathematics*, **5**, 57-70. <https://doi.org/10.22606/jaam.2020.52002>
 - [9] Zhao, F.Z. (2021) Predictive Continuum Constitutive Modeling of Unfilled and Filled Rubbers. *Journal of Advances in Applied Mathematics*, **6**, 144-159. <https://doi.org/10.22606/jaam.2021.63002>
 - [10] Lu, S.C.H. and Pister, K.S. (1975) Decomposition of Deformation and Representation of the Free Energy Function for Isotropic Thermoelastic Solids. *International Journal of Solids and Structures*, **11**, 927-934. [https://doi.org/10.1016/0020-7683\(75\)90015-3](https://doi.org/10.1016/0020-7683(75)90015-3)
 - [11] Pellicer, J., Manzanares, J.A., Zúñiga, J., Utrillas, P. and Fernández, J. (2001) Thermodynamics of Rubber Elasticity. *Journal of Chemical Education*, **78**, 263-267. <https://doi.org/10.1021/ed078p263>
 - [12] Rey, T., Chagnon, G., Le Cam, J.-B. and Favier, D. (2013) Influence of the Temperature on the Mechanical Behaviour of Filled and Unfilled Silicone Rubbers. *Polymer Testing*, **32**, 492-501. <https://doi.org/10.1016/j.polymertesting.2013.01.008>
 - [13] Fu, X.T., Wang, Z.P., Ma, L.X., Zou, Z.X., Zhang, Q.L. and Guan, X.X. (2020) Temperature-Dependence of Rubber Hyperelasticity Based on the Eight-Chain Model. *Polymers*, **12**, Article No. 932. <https://doi.org/10.3390/polym12040932>
 - [14] Staszczak, M., Pieczyska, E.A. and Maj, M., Urbański, L., Odriozola, I. and Martin, R. (2015) Thermomechanical Properties of Vulcanized Rubber Investigated by Testing Machine and Infrared Camera. *Measurement Automation Monitoring*, **61**, 206-209.
 - [15] Joule, J.P. (1859) V. On Some Thermo-Dynamic Properties of Solids. *Philosophical Transactions of the Royal Society*, **149**, 91-131. <https://doi.org/10.1098/rstl.1859.0005>
 - [16] Price, C. (1976) Thermodynamics of Rubber Elasticity. *Proceedings of the Royal Society of London*, **351**, 331-350. <https://doi.org/10.1098/rspa.1976.0145>
 - [17] Samaca Martinez, J.R., Le Cam, J.-B., Balandraud, X., Toussaint, E. and Caillard, J. (2013) Mechanisms of Deformation in Crystallizable Natural Rubber. Part 1: Thermal Characterization. *Polymer*, **54**, 2717-2726. <https://doi.org/10.1016/j.polymer.2013.03.011>

- [18] Le Cam, J.-B. (2018) Strain-Induced Crystallization in Rubber: A New Measurement Technique. *Strain*, **54**, e12256. <https://doi.org/10.1111/str.12256>
- [19] Pinter, C.C. (1990) A Book of Abstract Algebra. 2nd Edition, Dover Publications, Inc., Mineola, New York.
- [20] Noll, W. (1972) A New Mathematical Theory of Simple Materials. *Archive for Rational Mechanics and Analysis*, **48**, 1-50. <https://doi.org/10.1007/BF00253367>
- [21] Svendsen, B. (1998) A Thermodynamic Formulation of Finite-Deformation Elastoplasticity with Hardening Based on the Concept of Material Isomorphism. *International Journal of Plasticity*, **14**, 473-488. [https://doi.org/10.1016/S0749-6419\(98\)00002-3](https://doi.org/10.1016/S0749-6419(98)00002-3)
- [22] Bertram, A. (1999) An Alternative Approach to Finite Plasticity Based on Material Isomorphisms. *International Journal of Plasticity*, **15**, 353-374. [https://doi.org/10.1016/S0749-6419\(98\)00074-6](https://doi.org/10.1016/S0749-6419(98)00074-6)
- [23] Anthony, R.L., Gaston, R.H. and Guth, E. (1942) Equations of State for Natural and Synthetic Rubber-Like Materials. I. Unaccelerated Natural Soft Rubber. *The Journal of Physical Chemistry*, **46**, 826-840. <https://doi.org/10.1021/j150422a005>
- [24] Holzapfel, G.A. (2000) Nonlinear Solid Mechanics: A Continuum Approach for Engineering. 1st Edition, John Wiley & Sons Ltd., Chichester.
- [25] Candau, N., Chazeau, L., Chenal, J.-M., Gauthier, C., Ferreira, J., Munch, E. and Rochas, C. (2012) Characteristic Time of Strain Induced Crystallization of Crosslinked Natural Rubber. *Polymer*, **53**, 2540-2543. <https://doi.org/10.1016/j.polymer.2012.04.027>
- [26] Loos, K., Aydogdu, A.B., Lion, A., Johlitz, M. and Calipel, J. (2021) Strain-Induced Crystallisation in Natural Rubber: A Thermodynamically Consistent Model of the Material Behaviour Using a Serial Connection of Phases. *Continuum Mechanics and Thermodynamics*, **33**, 1107-1140. <https://doi.org/10.1007/s00161-020-00950-9>
- [27] Le Cam, J.-B. (2017) Energy Storage Due to Strain-Induced Crystallization in Natural Rubber: The Physical Origin of the Mechanical Hysteresis. *Polymer*, **127**, 166-173. <https://doi.org/10.1016/j.polymer.2017.08.059>